Unraveling the 1974 eruption of Fuego volcano (Guatemala) with small crystals and their young melt inclusions

Kurt Roggensack*
Department of Geology, Arizona State University, Tempe, Arizona 85287-1404, USA

ABSTRACT

This study demonstrates that crystal size may be used to temporally constrain melt inclusion data. This approach is applied to the 1974 Vulcanian-type eruption of Volcan Fuego in Guatemala to study magma conditions immediately prior to eruption. The 1974 ash deposit shows significant variations in matrix glass composition, crystal size, crystal content, and volatile (H_2O and CO_2) content in each of four eruptive phases occurring over a 10-day period. Matrix glass and melt inclusions hosted in small ($\sim$0.6 mg) olivine crystals have a particularly wide range in composition (basalt to andesite; 0.52–1.22 wt% K_2O) and a wide range in volatile saturation pressures ($\sim$1.0–4.4 kbar). That small (i.e., young) crystals host diverse melt inclusions demonstrates significant compositional variability in the magma system prior to eruption. The volatile saturation pressures indicate that magma was vertically distributed in the crust. During the eruption, different magmas from varying depths were hybridized, giving rise to short-term (hours to days) variation in the observed products.

Keywords: volatiles, decompression, degassing, hybridization, volcanic glass.

INTRODUCTION

If the age of individual melt inclusions could be determined, it would be possible to study the timing of dynamic magma processes such as decompression and magma mixing or to investigate the evolution of a single eruptive unit. One possibility is that the size of the host crystal could be used to delimit melt inclusion age, but this approach is complicated by the fact that melt inclusions could form at any time during crystal growth. It might be expected that a given crystal could host melt inclusions of variable age. The exception is young (i.e., small) crystals that may host only young melt inclusions. This simple relationship might be useful in two ways. First, melt inclusions hosted by small crystals provide information on late-stage magma processes. Second, contrasting the young melt inclusions in small crystals with variable-age melt inclusions in the moderate to large crystals should provide a more complete record of magma evolution. This report is an investigation of the first approach.

The 1974 eruption of Volcan Fuego, Guatemala, is among the most well-documented and well-studied mafic ash eruptions (Rose, 1977; Davies et al., 1978; Rose et al., 1978; Anderson, 1984; Harris and Anderson, 1984; Sisson and Grove, 1993). Direct observations coupled with sampling during and immediately after the eruption have allowed detailed comparisons between geochemical features and volcanic activity (e.g., Rose et al., 1978). Of particular interest has been the documentation of significant and variable water abundance in the 1974 Fuego magma (Sisson and Layne, 1993), variation in the phenocryst abundance, phase proportions, and melt inclusion compositions (Rose et al., 1978), and the identification of multiple plagioclase populations (Anderson, 1984). This study combines crystal size and melt inclusion analyses to identify the source of compositional and mineralogical variability in the 1974 deposit.

Current models of the 1974 eruption of Fuego involve decompression crystallization of a single magma body. Volatile saturation pressures from H_2O and CO_2 melt inclusion analyses and temporal restrictions imposed by crystal size show that the 1974 eruptive products were probably derived from several magmas. These data indicate that magma hybridization, rather than zoning of a single magma, is responsible for the previously documented variability in crystal and water content in the 1974 eruption.

MELT INCLUSION PREPARATION AND ANALYSIS

Individual olivine crystals from three of the four (first, second, and fourth) eruptive phases of the 1974 eruption (October 14, 17–18, and 23, respectively) were handpicked from ash, individually weighed, and mounted in epoxy. Minor contributions from glass selvage were ignored; mass corrections for broken crystals were based on visual shape estimates. Similarly, the mass of several earlier prepared crystals was estimated from crystal dimensions. Because crystal selection was in part based on size, the sample population is nonrandom, and no crystal size distribution analysis was attempted.

An optical microscope was used to locate melt inclusions (no hourglass or cracked varieties) in crystals. Melt inclusions were analyzed using the JEOL 8600 Superprobe at Arizona State University, calibrated with natural and synthetic standards operating at an accelerating voltage of 15 kV and 10 nA beam current. To minimize sodium loss in the hydrous glasses, the beam was defocused to 10 μm diameter, sodium was first in the analysis sequence, and counting times on peak and background were limited to 10 s. A focused beam was used for olivine analyses. All data were corrected using a ZAF routine.

Six melt inclusions were selected for analysis by Fourier transform infrared (FTIR) spectroscopy based on their small host-crystal size, which ensures a young melt inclusion age, and their presence in the earliest eruptive products. Each sample was double polished and thickness was measured with a Tencor alpha-step 200 profilometer. Spectra were collected using a Spectra Tech microscope, a Nicolet bench, and Omnic software. Backgrounds were subtracted by hand. The abundance of carbonate and water was calculated using the Beer-Lambert law and published extinction coefficients (Fine and Stolper, 1986; Dixon and Pan, 1995; Dixon et al., 1995).

---

*E-mail: kurt.roggensack@asu.edu.

Geology; October 2001; v. 29; no. 10; p. 911–914; 4 figures; 2 tables.

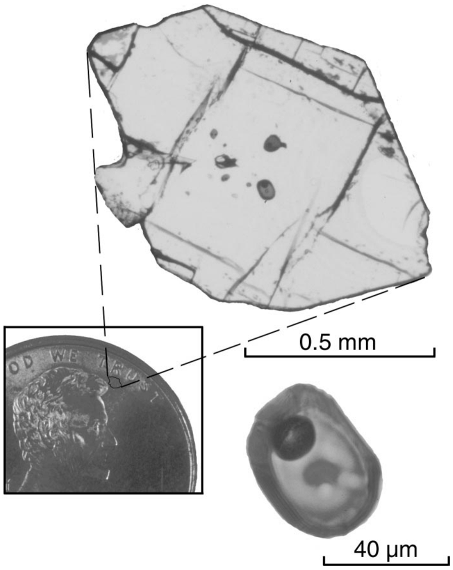

Figure 1. Photomicrographs of olivine crystal (19-5) erupted in opening phase of 1974 eruption of Fuego. Two melt inclusions are visible near center of crystal. Enlargement of lower melt inclusion contains typical vapor bubble (spot within inclusion is ion probe crater). Coin diameter is 19 mm.

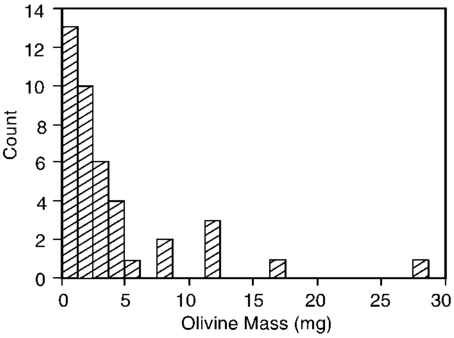

Figure 2. Range in olivine crystal mass from 1974 eruption of Fuego. About half of samples are from October 14 opening phase; remainder are from second and fourth eruptive phases.

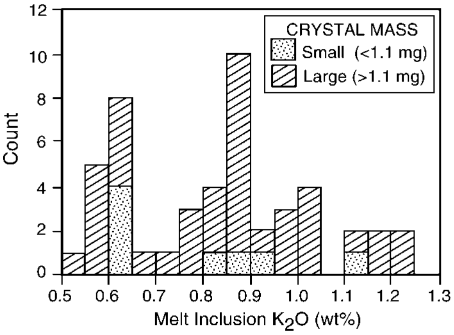

Figure 3. Compositional range of olivine melt inclusions.

CRYSTAL MASS AND MELT INCLUSION COMPOSITION

The 1974 eruption produced high-alumina basalt with phenocrysts of plagioclase, olivine, augite, magnetite, and oxyhornblende. Comparisons of the four eruptive phases show a general trend of increasing average crystal size and crystal abundance during the eruption (Rose et al., 1978). For example, olivine contents progressively increased (3.6% to 12.6% of total mineral volume), whereas plagioclase abundance fluctuated (21 to 31 vol%); the lowest values were during middle eruptive phases. The overall variation in crystal content and the variability of phenocryst proportions has been interpreted as zoning of a single magma body (Rose et al., 1978).

Olivine crystals are of special importance because they are relatively leak-proof melt inclusion hosts (e.g., Anderson and Brown, 1993). Olivine crystals from the 1974 Fuego ash are typically subhedral to euhedral (Fig. 1) and have resorbed areas along their margins, which are filled with magnetite, groundmass, or quenched glass. The olivine crystals display a large range in mass (≤28 mg), although generally crystals are <6 mg (Fig. 2).

The large compositional range for melt inclusions reported here (e.g., 0.52–1.22 wt% K_2O; Fig. 3) is virtually identical to earlier studies (0.59–1.33 wt% K_2O; Harris and Anderson, 1984). Within this compositional range the melt inclusions form an apparent bimodal distribution. One group of melt inclusions clusters near 0.60 wt% K_2O, whereas a second group clusters near 0.90 wt% K_2O. Matrix glass and glass reentrant analyses from early-erupted ash (~0.89 wt% K_2O; Table 1) are comparable to the second, evolved group of melt inclusions.

Rose et al. (1978) found that melt inclusions from a single scoria clast displayed as much compositional variation as the entire deposit. This feature, like the variation in crystal content, was interpreted as evidence of magma zoning. Newly acquired data indicate that the smallest, and presumably the youngest, olivine crystals (≤1.1 mg) host virtually the entire melt inclusion compositional range (0.62–1.13 wt% K_2O; Table 1).

Melt Inclusion Volatiles

FTIR analyses of melt inclusions hosted by small olivine crystals (≤1 mg) from early-erupted ash provide further information on late-stage magma conditions. The water content of these melt inclusions varies between

TABLE 1. MAJOR ELEMENT COMPOSITION OF ASH, MELT INCLUSIONS, AND MATRIX GLASS FROM 1974 ERUPTION OF FUEGO VOLCANO

Sample*	SiO_2	TiO_2	Al_2O_3	FeO†	MnO	MgO	CaO	Na_2O	K_2O	P_2O_5	S	Cl	Orig.	Fo§	Crystal mass# (mg)	Crystal length (mm)
Weighted average of entire eruption**																
	50.23	0.88	19.33	11.44	n.d.	4.98	8.98	3.39	0.76	n.d.	NA	NA	99.36	NA	NA	NA
Melt Inclusions																
19-5	51.14	0.79	18.92	9.96	0.26	4.80	9.82	3.46	0.62	0.22	0.17	0.11	95.21	74.9	0.68	1.0
19-33	58.11	0.89	16.56	8.13	0.15	4.17	6.15	4.45	1.13	0.26	0.15	0.17	95.86	72.8	1.10	1.1
19-38a	50.35	1.13	20.29	8.80	0.19	4.38	10.39	3.72	0.63	0.12	0.52	0.12	95.36	n.d.	0.58	n.d.
19-38b	50.11	1.00	20.22	8.82	0.11	5.17	10.23	3.57	0.63	0.15	0.47	0.12	95.80	77.3	0.58	n.d.
19-41	50.85	0.86	19.37	9.87	0.27	4.35	10.26	3.43	0.62	0.12	0.42	0.10	95.49	n.d.	1.11	1.1
19-51	53.62	1.18	17.86	9.67	0.14	4.10	8.05	4.21	0.90	0.26	0.25	0.13	96.13	n.d.	0.53††	n.d.
12-8a	53.10	1.20	17.69	10.32	0.15	3.09	9.18	4.13	0.88	0.27	0.30	0.14	94.45	n.d.	1.11	n.d.
12-8b	54.56	1.14	17.09	10.27	0.19	3.55	8.18	4.03	0.81	0.19	0.20	0.12	95.30	n.d.	1.11	n.d.
Matrix glass and reentrants																
19-RE	53.65	1.17	17.22	9.67	0.13	3.55	8.67	4.82	0.86	0.26	0.10	0.13	97.06	NA	NA	NA
19-41RE	54.93	1.19	16.95	9.51	0.16	3.83	7.85	4.45	0.89	0.24	0.25	0.14	95.15	NA	NA	NA
12-25MG	53.28	1.21	17.28	9.84	0.00	3.50	8.74	4.98	0.93	0.23	0.20	0.12	99.39	NA	NA	NA

Note: Orig.—original analysis total; analyses normalized to 100% on a volatile-free basis. NA—not applicable, n.d.—not determined. MG—matrix glass attached to crystal. RE—glass reentrant along crystal margin.

*Prefix indicates eruption date (19 is from first phase, 12 is from either first or second phase); a and b designate multiple melt inclusions within a single crystal.

†Total iron as FeO.

§Forsterite composition near (10 μm) melt inclusion.

#Mass of host crystal in milligrams; several crystals were corrected for minor breakage (~20% of total).

**From Rose et al. (1978).

††Aggregate of three small crystals.

3.1 and 4.8 wt%. Slightly higher water abundance (to 6.2 wt% H_2O) was measured in olivine melt inclusions by Sisson and Layne (1993), although the majority of their water analyses were within the range reported here. Melt inclusion CO_2 contents are also quite variable and combined with water indicate volatile saturation pressures of between 1.0 and 4.4 kbar. The highest volatile saturation pressures, in excess of 3 kbar, are found in melt inclusions with basalt compositions, whereas volatile saturation pressures are 2.5 kbar or less in basaltic andesite melt inclusions.

TABLE 2. MELT INCLUSION VOLATILES DETERMINED BY FOURIER TRANSFORM INFRARED SPECTROSCOPY

Sample*	Wafer thickness (μm)	OH (4500 cm^{-1}) (wt%)	H_2O mol (5200 cm^{-1}) (wt%)	H_2O mol (1630 cm^{-1}) (wt%)	$H_2O^{\dagger}_{Total}$ (wt%)	H_2O_{Total} (3500 cm^{-1}) (wt%)	CO_2 (ppm)	Saturation pressure (kbar)
19-5	46	2.5	2.2	2.0	4.7	3.9	762	3.7
19-33	50	2.3	2.5	2.6	4.8	4.0	159	2.5
19-38a	51	2.3	2.0	2.1	4.3	4.2	609	3.4
19-41	47	2.5	2.1	2.3	4.6	3.6	1249	4.4
19-51	30	n.d.	n.d.	2.4	n.d.	3.1	b.d.l.	1.0
12-8a	42	n.d.	n.d.	2.1	n.d.	3.6	b.d.l.	1.4

Note: n.d.—not determined; b.d.l.—below detection limit (~50 ppm); assume 2.6 g/cm^3 glass density.
*Sample suffixes (a, b) same as in Table 1.
†Sum of 4500 cm^{-1} and 5200 cm^{-1} data.

DISCUSSION

Crystal Fractionation

Before considering crystal fractionation it is important to consider the possible influence of postentrapment crystallization on melt inclusion compositions. Addition of olivine (1% increments) assuming a $K_D^{Fe\text{-}Mg}$ of 0.32 shows that the potential amount of postentrapment crystallization varies between 0% and 10%. This result is consistent with earlier studies (Harris and Anderson, 1984; Sisson and Layne, 1993) and indicates that postentrapment crystallization has had a negligible effect on Fuego melt inclusion compositions.

The compositional variation in Fuego's melt inclusions most likely reflects significant amounts of crystal fractionation (~50% for K_2O 0.60–1.13 wt%). There is a general consensus among previous investigators that removal of the observed mineral assemblage of plagioclase, olivine, clinopyroxene, and magnetite could produce the compositional range observed in melt inclusions (Rose et al., 1978; Harris and Anderson, 1984; Sisson and Layne, 1993). Although the modal abundance of clinopyroxene is low relative to the cotectic (Sisson and Grove, 1993) and fractionation models (Rose et al., 1978; Harris and Anderson, 1984), the discrepancy probably reflects expansion of plagioclase and olivine phase volumes during decompression and loss of water (Sisson and Layne, 1993).

Crystal Size and the Case for Hybridization

Determining the time of geologic processes, especially the short time scales of volcanic processes, presents a significant challenge. Previous studies have shown how mineral breakdown (Rutherford, 1993), crystal content in an eruption series (Cashman and Taggart, 1983; Melson, 1983), and microlites (Hammer et al., 1999) can be used to study magma crystallization and decompression on short time scales (hours to months). At Fuego the question is whether it is possible to discriminate between petrologic features that pre-date the eruption and those that were coeval with the eruption.

Crystal size can be used to identify young melt inclusions. The small olivine crystals (~1.1 mm long) from the 1974 eruption of Fuego are roughly 127 days old, if we assume an olivine growth rate of 10^{-8} cm/s (Jambon et al., 1992). Small crystals that host compositionally diverse melt inclusions in the Fuego ash reflect significant diversity in the magma system immediately prior to the eruption. This result could be consistent with magma zoning (Rose et al., 1978) or in situ crystallization (Harris and Anderson, 1984), although the vertical distribution of the magma must also be considered.

Volatile saturation pressures of melt inclusions provide a spatial framework for Fuego's magma. Evidence from the young (small) Fuego olivine crystals indicates that magma compositions varied with depth. The highest volatile saturation pressures are found in low-K_2O melt inclusions. As volatile saturation pressures decrease, the melt inclusion K_2O contents increase. Superficially, this relationship resembles a magma decompression trend, and it indicates that the compositional variation in melt inclusions developed over a range of depth.

Consideration of crystal size relationships indicates that it is unlikely that the Fuego data represent a single-stage process of magma decompression. The range in volatile saturation pressures is consistent with decompression in the range of 1–4.4 kbar (3–13 km depth range). This magnitude of decompression would strongly promote crystallization of a volatile-rich magma. With the possible exception of rapid magma ascent, crystal size should show some relationship to decompression history. Crystals that have undergone the greatest decompression should be largest. Instead, young crystals of identical mass (~0.6 mg) show contrasting saturation pressures and major element compositions (Tables 1 and 2). It can be concluded that the 1974 Fuego deposit represents a hybrid formed from several magmas at variable depth. The bimodal distribution of melt inclusion compositions (Fig. 3) and the saturation pressure relationships are consistent with a predominantly basaltic magma (~0.60 wt% K_2O) at >10 km depth (>3 kbar) and a second basaltic andesite magma (~0.90 wt% K_2O) at 3–8 km depth (1.0–2.5 kbar).

Hybridization could also explain other features of the 1974 ash deposit. For example, (1) short-term variation in crystal content and mineral proportions during the eruption, (2) multiple plagioclase populations (Anderson, 1984), and (3) the juxtaposition of diverse melt inclusions, reflecting as much as ~50% crystallization, within a single scoria lump (Rose et al., 1978) could be explained by hybridization. Although flow segregation, plagioclase flotation, and magma zoning (wall contact versus interior) may have also contributed to the Fuego variation, the spatial (volatile saturation pressures) and temporal (crystal size) data are compatible with a compositionally diverse, vertically distributed magma system. On the basis of the crystal size relationships, I speculate that magma hybridization occurred relatively late (immediately before or during eruption) rather than during an earlier event (e.g., recharge; Davidson and Tepley, 1997). The oscillatory zoned margins and sodic rims of plagioclase phenocrysts (Anderson, 1984) are consistent with this interpretation.

CONCLUSIONS

Crystal size can be used as a temporal limitation for melt inclusion studies. Small, young olivine crystals from the Fuego eruption contain melt inclusions that demonstrate that magma was distributed over considerable crustal depth (~3–13 km) prior to the eruption. Either immediately before or during the eruption, magmas from different depths combined to form a hybrid (Fig. 4). This finding has significant implications for the interpretation of the deposit. For example, bulk compositions, mineral modes, and the large variation in water abundance reflect the contribution of several magmas rather than a single magma composition. This type of cryptic hybridism might be a common character-

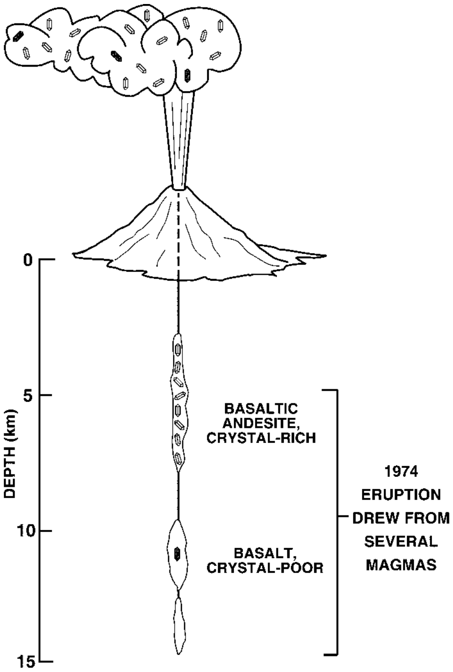

Figure 4. Schematic representation of 1974 Fuego eruption. Olivine crystals were sampled from two magmas.

istic of mafic arc magmas. Because the magmas are likely to have a common source, few other geochemical parameters (stable or radiogenic isotopes, bulk analyses of trace or minor elements) have the power to illuminate this process better than melt inclusions from small crystals.

ACKNOWLEDGMENTS

I thank S. Bonis for sampling and recording the events of the 1974 eruption; W.I. Rose for providing access to his sample collection and notes on the 1974 eruption (National Science Foundation [NSF] DES 7419025); J. Clark for assistance on the Arizona State University electron probe (obtained with aid from National Science Foundation grant EAR-8408163); J. Lowenstern (U.S. Geological Survey) for access to his Fourier transform infrared laboratory; R.L. Hervig and J.H. Fink for helpful comments; and Sue Selkirk for help with figure preparation. Partial funding was provided by National Science Foundation grant EAR-9706263. I thank W.I. Rose and T.A. Vogel for constructive reviews.

REFERENCES CITED

Anderson, A.T., 1984, Probable relations between plagioclase zoning and magma dynamics, Fuego volcano, Guatemala: American Mineralogist, v. 69, p. 660–676.

Anderson, A.T., and Brown, G.G., 1993, CO_2 contents and formation pressures of some Kilauean melt inclusions: American Mineralogist, v. 78, p. 794–803.

Cashman, K.V., and Taggart, J.E., 1983, Petrologic monitoring of 1981 and 1982 eruptive products from Mount St. Helens: Science, v. 221, p. 1385–1387.

Davidson, J.P., and Tepley, F.J., 1997, Recharge in volcanic systems: Evidence from isotope profiles of phenocrysts: Science, v. 275, p. 826–829.

Davies, D.K., Quearry, M.W., and Bonis, S.B., 1978, Glowing avalanches from the 1974 eruption of the volcano Fuego, Guatemala: Geological Society of America Bulletin, v. 89, p. 369–384.

Dixon, J.E., and Pan, V., 1995, Determination of the molar absorptivity of dissolved carbonate in basanitic glass: American Mineralogist, v. 80, p. 1339–1342.

Dixon, J.E., Stolper, E.M., and Holloway, J.R., 1995, An experimental study of water and carbon dioxide solubilities in mid-ocean ridge basaltic liquids. Part I: Calibration and solubility results: Journal of Petrology, v. 36, p. 1607–1631.

Fine, G.J., and Stolper, E., 1986, Carbon dioxide in basaltic glasses: Concentrations and speciation: Earth and Planetary Science Letters, v. 76, p. 263–278.

Hammer, J.E., Cashman, K.V., Hoblitt, R.P., and Newman, S., 1999, Degassing and microlite crystallization during pre-climactic events of the 1991 eruption of Mt. Pinatubo, Philippines: Bulletin of Volcanology, v. 60, p. 355–380.

Harris, D.M., and Anderson, A.T., 1984, Volatiles H_2O, CO_2, and Cl in a subduction related basalt: Contributions to Mineralogy and Petrology, v. 87, p. 120–128.

Jambon, A., Lussiez, P., Clocchiatti, R., Weisz, J., and Hernandez, J., 1992, Olivine growth rates in a tholeiitic basalt: An experimental study of melt inclusions in plagioclase: Chemical Geology, v. 96, p. 277–287.

Melson, W.G., 1983, Monitoring the 1980–1982 eruptions of Mount St. Helens: Compositions and abundances of glass: Science, v. 221, p. 1387–1391.

Rose, W.I., 1977, Scavenging of volcanic aerosol by ash: Atmospheric and volcanologic implications: Geology, v. 5, p. 621–624.

Rose, W.I., Anderson, A.T., Woodruff, L.G., and Bonis, S.B., 1978, The October 1974 basaltic tephra from Fuego volcano: Description and history of the magma body: Journal of Volcanology and Geothermal Research, v. 4, p. 3–53.

Rutherford, M.J., 1993, Experimental petrology applied to volcanic processes: Eos (Transactions, American Geophysical Union), v. 74, p. 49, 55.

Sisson, T.W., and Grove, T.L., 1993, Temperatures and H_2O contents of low-MgO high-alumina basalts: Contributions to Mineralogy and Petrology, v. 113, p. 167–184.

Sisson, T.W., and Layne, G.D., 1993, H_2O in basalt and basaltic andesite glass inclusions from four subduction-related volcanoes: Earth and Planetary Science Letters, v. 117, p. 619–635.

Manuscript received January 22, 2001
Revised manuscript received May 8, 2001
Manuscript accepted May 21, 2001

Printed in USA